# 5 GHz Intra-Vehicle Channel Characterization

David W. Matolak

School of EECS, Ohio University
Athens, Ohio USA 45701
email: matolak@ohio.edu

Arvind Chandrasekaran

Photon Infotech
100 Century Center Court, San Jose, California USA
email: chandrasekaran.arvind@gmail.com

***Abstract*—This paper presents wideband wireless channel characterization results for intra-automobile communication in the 5 GHz band. Results pertain to data collected from a mini-van and bus, both parked. Motivating this work is the scarcity of results for intra-automobile wireless channel characteristics. This paper describes some related work, the measurement conditions and procedures, and resulting channel characteristics for the two environments. Measurements were taken using a 50 MHz bandwidth spread spectrum correlator channel sounder, and power delay profiles (PDPs) were collected. We provide root-mean square delay spread (RMS-DS) statistics, and statistical channel models for these two intra-automobile channels. Mean RMS-DS values are approximately 17 ns in the mini-van, and 17 and 22 ns for measurements with two different transmitter locations in the bus. RMS-DS standard deviations range from 2-6 ns. As expected, the RMS-DS values increase with vehicle size and transmitter-receiver distance. Both human movement and the unique physical structures of the intra-automobile environment also strongly affect the channel's characteristics.**

## I. Introduction

Vehicle-to-vehicle (V2V) communications has seen much attention in recent years, e.g., [1]-[4]. Topics addressed include channel modeling [5]-[8], medium access control [9], standards [10]-[11], and others. Applications include road safety warnings, reduction of energy use, traffic efficiency increases, and personal services ("comfort" or "infotainment" applications). Some applications employ local transceivers at roadsides, and these are classed as vehicle-to-roadside (V2R) or vehicle-to-infrastructure (V2I) communication.

Communications *within* vehicles is also of interest, as sensors are being used to monitor an ever-increasing number of parameters associated with automotive health, safety, and performance. Traditionally these sensors were connected via wires, but as the number and complexity of the systems increases, the use of wireless sensors is becoming more attractive for their ease of installation and maintenance, and reduced cost [12] compared to wired systems.

Sensor locations occur throughout the vehicle, and can be in the engine compartment, wheel wells, trunk, and passenger cabin. Our focus here is on the passenger cabin, so our results can have application not only to sensor communication within the passenger cabin, but also to communication between passenger-deployed devices operating in the 5 GHz frequency band of our measurements.

Prior work on intra-vehicle channels is sparse. The authors of [13] reported results for ultrawideband (UWB) performance with transmitter (Tx) and receiver (Rx) located in various sections of an automobile. The UWB pulses were "baseband," with a pulse width of approximately 300 ps, corresponding to a bandwidth of approximately 3.33 GHz. Antenna and spectral characteristics were not provided. Reference [13] also did not report statistical channel characteristics, as we do here.

In [14]-[16] the authors characterized the wireless channel within aircraft of various sizes, and reported delay spreads and path losses, as well as statistics for the number of multipath components. Reference [14] used the UMTS band (~2 GHz), [15] the 5 GHz band, and [16] a UWB signal. In [17] the author found "hyper-Rayleigh" (worse than Rayleigh, or "severe") fading in a number of vehicles: two fixed-wing and one non fixed-wing aircraft, and a bus. Results pertain to the 2.4 GHz band. Only narrowband fading distributions were given in [17]. The authors of [18] provide narrowband amplitude fading data for an intra-automobile channel, in the 2.4 GHz band. Although [16] provides some delay spread values (for aircraft) and [14] provides sufficient data for modeling the intra-aircraft channel in the UMTS band, there is little work to be found on intra-car channel models. Other than our work in [19] which we report here, no explicit models or wideband results appear to be available for the intra-automobile (or intra-bus) channel in the 5 GHz band, with the exception of [20]. In [20], the authors use a UWB signal of bandwidth 200 MHz, centered at 5 GHz. Root-mean square delay spreads (RMS-DS) of approximately 11 ns were reported, from power delay profile (PDP) measurements. These PDPs were related to results obtainable in a reverberation chamber, but insufficient detail is given in [20] to construct a channel model.

In this paper we add to the results on intra-vehicle channel characterization, specifically for the 5 GHz band, and for both a passenger vehicle (mini-van) and a commercial bus. We provide results for the vehicles parked, with other vehicles and buildings nearby. Our results are for "mostly empty" vehicles, but we also characterize the effect of human presence and movement upon delay spreads in the bus.

In Section II, we describe the vehicles and the measurement parameters. Section III contains measured channel results and our derived channel models. In Section IV we provide conclusions.

978-1-4673-1881-5/12/$31.00 ©2012 IEEE

## II. VEHICLE AND MEASUREMENT DESCRIPTION

For our study, we conducted measurements within two vehicles. All measurements were in the 5 GHz band, at a center frequency of 5.22 GHz.

### A. *Vehicles*

The van measurements were conducted in a 2001 Honda Odyssey mini-van. The Honda odyssey is a regular seven-seat passenger mini-van. The bus measurements were carried out in a general purpose Ohio University passenger air-bus. The bus, manufactured by Van Hool, is a fifty five-seat air-bus. Both vehicles have an external metallic body. The external dimensions of the mini-van and bus are listed in Table I.

TABLE I. EXTERNAL DIMENSIONS OF HONDA ODYSSEY MINI-VAN AND PASSENGER BUS (METERS)

| DIMENSION | VAN | BUS |
|---|---|---|
| Length | 5.13 | 13.72 |
| Width | 1.78 | 2.59 |
| Height | 1.96 | 3.62 |

The van was parked in a parking lot with approximately 50 other vehicles in the vicinity within a thirty meter radius. In addition to the vehicles, there were buildings at distances of approximately thirty-forty meters. These metallic and brick structures contributed some longer-delay, but substantially weaker, multipath reflection signals. Figure 1 shows a photograph of the van local environment.


Fig. 1. External environment for van measurements.

The bus was surrounded by about 25 other cars and vans in the parking lot within about thirty meters. The bus was parked within ten meters of the metallic parking garage due to space restrictions. In addition, there was a thirty-meter tall chimney at a distance of approximately forty meters and other buildings at distances of about fifty meters as shown in Figure 2.

Measurements were taken in three different locations in the van; in the front seat (Rx 1), rear seat (Rx 2) and in the trunk (Rx 3). The transmitter was located on the dashboard. Both transmitter and receiver antenna were kept stationary during measurements. There was one person inside the van in the front seat recording data. Once data was successfully collected from one position, the receiver was moved to the next position for measurements.


Fig. 2. Bus measurements external environment (nearby cars not shown).

In the bus, we took measurements in five receiver locations. Two transmitter locations were used in order to assess the effect of transmitter location on the bus channel. The first transmitter position (Tx 1) was in the front of the bus, right next to the driver on the dashboard. This position characterizes the channel from the driver terminal to the passengers. The three receiver positions were at varied distances from the transmitter in the front (Rx 1), middle (Rx 2) and rear passenger seats (Rx 3). The second transmitter position (Tx 2) was in the middle of the bus on the inside roof and the two receiver positions were in the back (Rx 4) and front (Rx 5) of the bus. This position of the transmitter enables characterization of the channel for passenger-to-passenger data transfer. The different transmitter and receiver locations in the van and bus are shown in Figures 3 and 4.

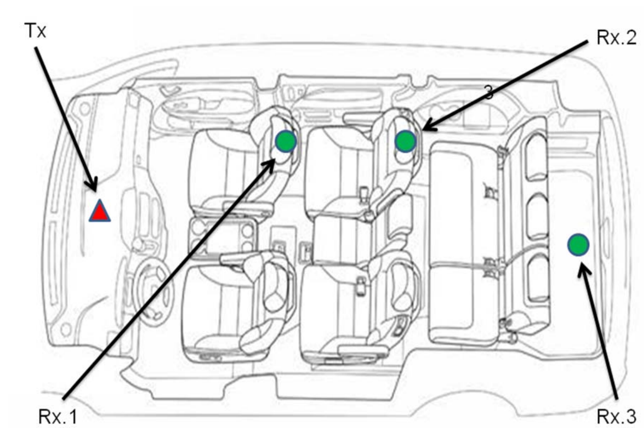


Fig. 3. Transmitter and receiver locations in van.

Link distances for all measurements are provided in Table II. All vehicle doors and windows were closed during measurements. Also, within the bus we took measurements with both no passenger movement, and with (7) moving passengers. Passengers within the bus sat in various locations throughout measurements.

### B. *Measurements*

The measurement test equipment consists of the Tx and Rx, collectively termed the "sounder." Our sounder was custom-manufactured by Berkeley Varitronics Systems [21]. The sounder is a spread spectrum stepped correlator, with

TABLE II. LINK DISTANCES (METERS) FOR VAN AND BUS.

| RX LOCATION | LINK DISTANCE | |
|---|---|---|
| VAN | | |
| Front seat (Rx 1) | 1.2 | |
| Rear seat (Rx 2) | 2.1 | |
| Trunk (Rx 3) | 3.4 | |
| BUS | | |
| | DASHBOARD TX | ROOF TX |
| Front Seat (Rx 1) | 3.0 | — |
| Middle Seat (Rx 2) | 7.6 | — |
| Rear Seat (Rx 3) | 12.8 | — |
| Rear Seat (Rx 4) | — | 7.6 |
| Dashboard (Rx 5) | — | 5.2 |

Fig. 4. Transmitter and receiver locations in bus.

adjustable center frequency within the 5 GHz band. The sounder elements are portable, and both Tx and Rx can be powered by battery to enable mobile measurements. The sounder's main features appear in Table III.

TABLE III. CHANNEL SOUNDER AND MEASUREMENT SYSTEM PARAMETERS

| CHARACTERISTIC | VALUE |
|---|---|
| Transmit power | +5 to 33 dBm |
| Center frequency | 5.12-5.22 GHz |
| Chip rate | 50 Mcps |
| Unambiguous delay range | 5.1 $\mu$sec |
| Bandwidth (99% power) | 52.76 MHz |
| Measurement rate | 2-60 PDPs/sec |
| Antennas | Omni monopoles, gain 1.5 dBi, polarization vertical |

Transmit power level is adjustable; we used the maximum value of 33 dBm to ensure a large signal-to-noise ratio at the Rx. The measurements provide power delay profiles (PDPs), which enable generation of channel impulse response (CIR) estimates (phases were also measured). Once calibrated, Tx and Rx are detached and moved to their locations for measurements.

PDPs were collected from each location for approximately 20-30 seconds. Approximately 1100 PDPs were collected in total for the van measurements in the three different Rx positions (since the channel was essentially time-invariant, good estimates of RMS-DS are obtained with a few hundred PDPs). For the bus measurements, during the first 10-15 seconds there was no human movement and during the second 10-15 seconds, there was human movement. Seven people moved inside the bus during the second half of the measurement for each receiver location. Approximately 3600 PDPs and 1675 PDPs were collected from the first and second transmitter bus positions, respectively.

After data conversions, the CIR magnitude and phase data was imported to MATLAB® to compute statistical channel parameters from the PDPs. A noise thresholding algorithm [22] was applied to ensure that the probability of mistaking a noise component for a multipath component (MPC) was less than $2\times10^{-3}$. All PDPs were also thresholded to exclude weak MPCs that were 25 dB or more below the PDP peak.

## III. Measured Results and Models

In this section, we describe the measured channel statistics, including RMS-DS and its distribution and variation. We also provide tapped-delay line channel models based on the PDPs collected over time.

### A. Measurement Results

The PDPs were processed to estimate RMS-DS, the most common measure of temporal dispersion. The RMS-DS, $\sigma_\tau$, is

$$\sigma_\tau = \sqrt{\left\{\left[\sum_{k=0}^{L-1}\tau_k^2\alpha_k^2\right] / \sum_{k=0}^{L-1}\alpha_k^2\right\} - \mu_\tau^2} . \quad (1)$$

In (1), the $\alpha$'s and $\tau$'s are respectively the amplitudes and delays of the measured MPCs, $L$ is the number of MPCs, and mean energy delay $\mu_\tau$ is given by

$$\mu_\tau = \left[\sum_{k=0}^{L-1}\tau_k\alpha_k^2\right] / \sum_{k=0}^{L-1}\alpha_k^2 . \quad (2)$$

All measured phases were found to be well modeled as uniformly random on [0, 2π).

Table IV provides aggregate RMS-DS statistics for all cases. These pertain to the "instantaneous" RMS-DS, where (1) is computed for each individual PDP, and the statistics are collected over the set of instantaneous RMS-DS values.

A histogram of instantaneous RMS-DS for the van is shown in Figure 5. RMS-DS histograms for the two bus transmitter locations are shown in Figures 6 and 7. An example PDP for the bus appears in Figure 8; samples are separated in delay by the reciprocal of measurement bandwidth, 20 ns. (Noise samples have not been discarded in this plot.) Note in Figure 8 the "rise time" of the PDP corresponding to attenuated samples through/around passengers and seats, then the peak sample, then subsequent samples with roughly exponentially decreasing power. Note also that bulk (group) delay has not been scaled accurately, i.e., the PDP is shifted to the center for visual clarity.

TABLE IV. RMS-DS STATISTICS FOR ALL VEHICLES (NS)

| VEHICLE | RMS-DS STATISTIC | | |
|---|---|---|---|
| | MIN/MAX | MEAN | STANDARD DEVIATION |
| Bus (Rx 1, 2, 3) | 3.81/35 | 17.05 | 5.36 |
| Bus (Rx 4, 5) | 5.45/31 | 22.45 | 4.54 |
| Van | 7.39/21 | 16.63 | 2.29 |

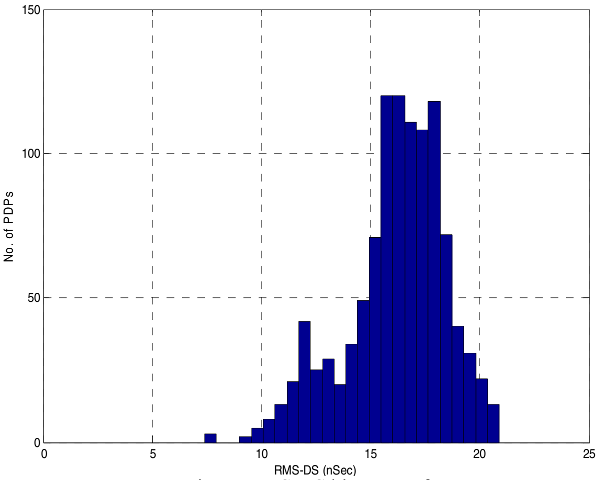

Fig. 5. RMS-DS histogram for van.

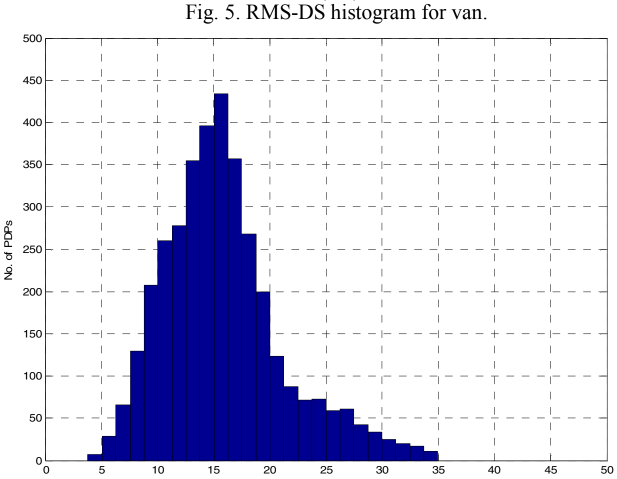

Fig. 6. RMS-DS histogram for bus, Tx 1 (Rx 1, 2, 3).

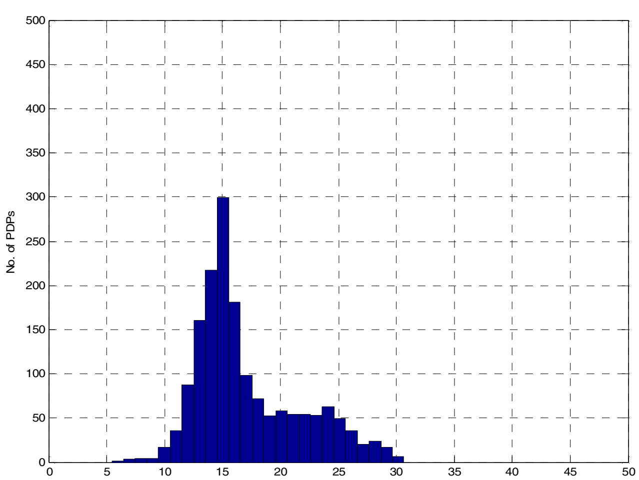

Fig. 7. RMS-DS histogram for bus, Tx 2 (Rx 4, 5).

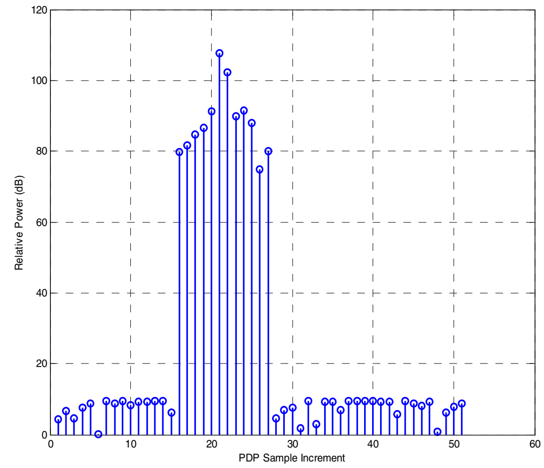

Fig. 8. Example PDP from bus, Tx location 2. RMS-DS=29 ns.

The effect of passenger movement on the RMS-DS in the bus is illustrated in Figure 9. This figure plots RMS-DS vs. PDP index (time). PDPs were taken at a rate of approximately 12/second. As previously noted, during the first half of measurements at each location, all passengers were motionless; during the second half of the measurement period, the 7 bus passengers moved in the aisles, and in and out of various seats. The effect on RMS-DS is clear for both Tx locations. Passenger motion not only causes more variation in RMS-DS, but can also increase its value. An increase occurs because much of the line-of-sight component energy can be blocked by the human body. In the case of Rx location 5, RMS-DS is approximately 15 ns in the motionless case, and can double when passengers are in motion.

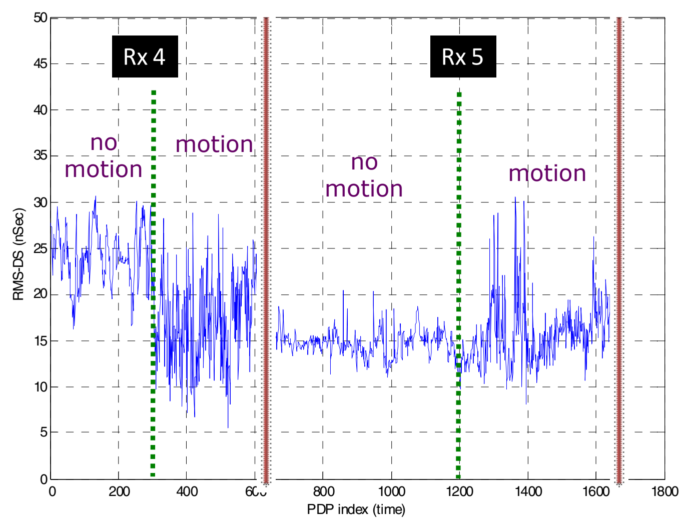

Fig. 9. RMS-DS vs. time for bus, Tx 2 (Rx 4, 5).

*B. Channel Models*

Even though the van channel is mostly time-invariant, some slow variation occurs due to passenger motion, and to a lesser degree from motion outside the vehicles. This is true as well for the bus.

We employ the popular tapped delay line model for our statistical intra-vehicle channel models. For this, we specify the number of taps ($L$), and the tap energies and amplitude fading parameters. The number of taps is based upon the mean value of RMS-DS; inter-tap spacing is 20 ns in delay.

Table V provides the channel parameters. We use the flexible Weibull distribution [23] to model the moderate amplitude fading on the taps (non-first-tap measured phases were well modeled as uniform). The Weibull $\beta$ factor is analogous to a Ricean $K$-factor, with $\beta$=2 constituting Rayleigh fading, and $\beta$>2 more benign conditions. (The Weibull scale factor can be derived from $\beta$ and tap energy.)

TABLE V. CHANNEL TAP PARAMETER STATISTICS, ALL VEHICLES.

| VEHICLE | TAP INDEX | TAP ENERGY | WEIBULL SHAPE FACTOR (β) |
|---|---|---|---|
| Van | 1 | 0.80 | 13.71 |
| | 2 | 0.20 | 3.96 |
| Bus (Rx 1, 2, 3) | 1 | 0.84 | 8.17 |
| | 2 | 0.16 | 2.0 |
| Bus (Rx 4, 5) | 1 | 0.745 | 11.13 |
| | 2 | 0.191 | 1.85 |
| | 3 | 0.064 | 1.63 |

As observed from Table V, fading is nearly non-existent in the van, and on the first taps of all channels. The second and third taps for the bus channels do though show some severe fading conditions, and this is ascribed to the passenger motion. (When passengers are motionless, the Weibull $\beta$ factor on these taps is typically 4 or larger). Figure 10 shows a histogram and probability density function (pdf) ML fits to the data for tap 3 in the bus. The Nakagami distribution with $m$-factor of approximately 0.66 also fits the severe fading well.

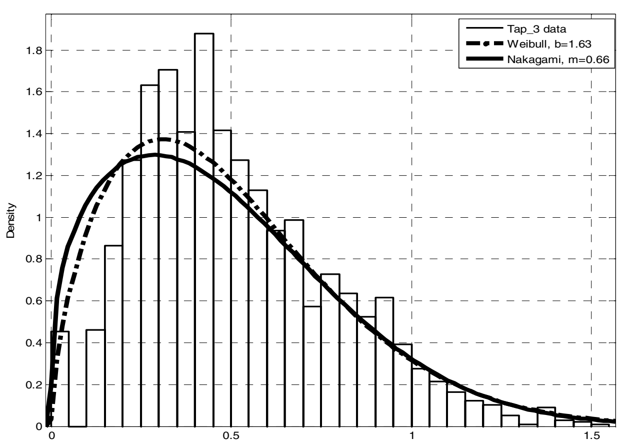

Fig. 10. Histogram & two pdf fits, bus fading tap #3 amplitude, Tx 2 (Rx 4, 5).

## IV. CONCLUSION

In this paper, we have presented results from intra-vehicle channel measurements in the 5 GHz band, for a mini-van and bus. Power delay profiles were measured for a variety of receiver locations, and RMS-DS was computed. Mean RMS-DS values in the van are approximately 17 ns, and in the bus, approximately 17-22 ns, depending on transmitter and receiver position. We also provided tapped-delay line channel models for these two intra-vehicle environments, and found some severe fading due to passenger motion. The effect of this motion (increasing RMS-DS) also constitutes some new findings for this environment. Future work includes additional measurements with vehicles in motion.

## REFERENCES


[1] ITS project website, http://www.its.dot.gov/index.htm, February 2007.

[2] *IEEE Vehicular Technology Magazine*, Special Issue on V2V Communications, vol. 2, no. 4, December 2007.

[3] S. Biswas, R. Tatchikou, F. Dion, "Vehicle-to-Vehicle Wireless Communication Protocols for Enhancing Highway Traffic Safety," *IEEE Comm. Mag.*, vol. 44, no. 1, pp. 74-82, January 2006.

[4] G. Karagiannis, O. Altintas, E. Ekici, G. Heijenk, B. Jarupan, K. Lin, T. Weil, "Vehicular Networking: A Survey and Tutorial on Requirements, Architectures, Challenges, Standards, and Solutions," *IEEE Comm. Surveys & Tutorials*, vol. 13, no. 4, pp. 584-616, Fourth Quarter 2011.

[5] G. Acosta-Marum, M. A. Ingram, "Six Time- and Frequency-Selective Empirical Channel Models for Vehicular Wireless LANs," *IEEE Vehicular Technology Mag.*, vol. 2, no. 4, pp. 4-11, December 2007.

[6] I. Sen, D. W. Matolak, "Vehicle-Vehicle Channel Models for the 5 GHz Band," *IEEE Trans. Intelligent Transportation Systems*, vol. 9, no. 2, pp. 235-245, June 2008.

[7] D. W. Matolak, Q. Wu, I. Sen, "5 GHz Band Vehicle-to-Vehicle Channels: Models for Multiple Values of Channel Bandwidth," *IEEE Trans. Vehicular Tech.*, vol. 59, no. 5, pp. 2620-2625, June 2010.

[8] J. Karedal, F. Tufvesson, N. Czink, A. Paier, C. Dumard, T. Zemen, C. F. Mecklenbrauker, A. F. Molisch, "A Geometry-Based Stochastic MIMO Model for Vehicle-to-Vehicle Communications," *IEEE Trans. Wireless Comm.*, vol. 8, no. 7, pp. 3646-3657, July 2009.

[9] J. Zhu, S. Roy, "MAC for Dedicated Short Range Communications in Intelligent Transportation," *IEEE Comm. Mag.*, vol. 41, no. 12, pp. 60-67, December 2003.

[10] D. Jiang, L. Delgrossi, "IEEE 802.11p: Towards an International Standard for Wireless Access in Vehicular Environments," *IEEE Int. Symp. on Wireless Vehicular Comm. (WiVec)*, Calgary, CA, Sept. 2008.

[11] R. Uzcategui, G. Acosta-Marum, (2009) WAVE: A Tutorial," *IEEE Comm. Mag.*, vol. 47, no. 5, pp. 126-133, May 2009.

[12] G. Leen, D. Heffernan, "Vehicles Without Wires," *Comput. Control Eng. Journal*, vol. 12, no. 5, pp. 205-211, Oct. 2001.

[13] J. Li, T. Talty, "Channel Characterization for Ultra-Wideband Intra-Vehicle Sensor Networks," *Proc. IEEE Military Communications Conference,* Washington, DC, 23-25 October 2006.

[14] N. R. Diaz, J. E. Esquitino, "Wideband Channel Characterization for Wireless Communication Within Short Haul Aircraft," *Proc. IEEE Spring Vehicular Tech. Conf.*, Milan, IT, 17-19 May 2004.

[15] D. W. Matolak, A. Chandrasekaran, "Aircraft Intra-Vehicular Channel Characterization in the 5 GHz Band," *Proc. 8th AIAA/IEEE Integrated Communications, Navigation, and Surveillance Conf.*, Bethesda, MD, 5-7 May 2008.

[16] A. P. G. Ariza, R. Zetik, S. Guowei, R. Muller, R. S. Thoma, M. Bachhuber, R. Weighl, T. Airbus, "Ultrawideband Channel Sounding within an Airbus 319," *Proc. IEEE Fall Vehicular Tech. Conf.*, Ottawa, ON, Canada, 6-9 September 2010.

[17] J. Frolik, "A Case for Considering Hyper-Rayleigh Fading Channels," *IEEE Trans. Wireless Comm.*, vol. 6, no. 4, pp. 1235-1239, April 2007.

[18] A. R. Moghimi, H-M Tsai, C. U. Saraydar, O. K. Tonguz, "Characterizing Intra-Car Wireless Channels," *IEEE Trans. Vehicular Tech.*, vol. 58, no. 9, pp. 5299-5305, November 2009.

[19] A. Chandrasekaran, "Intra-Vehicle Channel Characterization in the 5 GHz Band," Master's Thesis, Ohio University School of EECS, March 2011.

[20] O. Delangre, S. Van Roy, P. De Doncker, M. Lienard, P. Degauque, "Modeling In-vehicle Wideband Wireless Channels using Reverberation Chamber Theory," *Proc. 1st IEEE Workshop on Wireless Vehicular Comm.*, Baltimore, MD, 30 Sep.-1 Oct. 2006.

[21] Berkeley Varitronics Systems, Inc., website, http://www.bvssystems.com, January 2012.

[22] E. S. Sousa, V. M. Jovanoic, C. Daigneault, "Delay Spread Measurements for the Digital Cellular Channel in Toronto," *IEEE Trans. Veh. Tech.*, vol. 43, no. 4, pp. 837-847, Nov. 1994.

[23] A. Papoulis, U. Pillai, *Probability, Random Variables, and Stochastic Processes*, 4th ed. New York: McGraw-Hill, 2001.